A porous chiral In-MOF with anionic-type diamond network: synthesis, structure and nitrogen gas adsorption

Liping Wang,[a] Tianyou Song,[a] Liangliang Huang,[a] Jianing Xu,*[b] Chao Li,[a] Caixia Ji,[a] Liang Shan[a] and Li Wang*[a]

Received (in XXX, XXX) Xth XXXXXXXXX 20XX, Accepted Xth XXXXXXXXX 20XX
DOI: 10.1039/b000000x

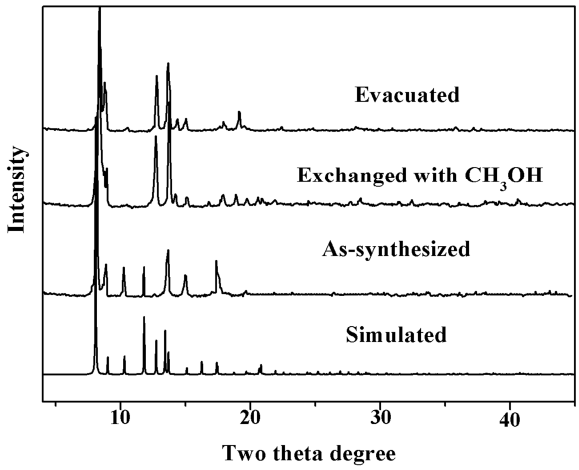

Fig. S1. Simulated, as-synthesized, exchanged with methanol, and evacuated at 80 ^{o}C overnight powder X-ray diffraction patterns for **1**.

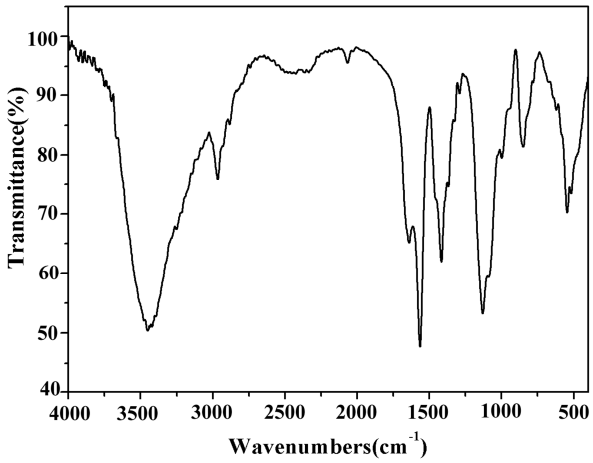

Fig. S2. The IR spectrum for **1** in the region 4000 – 400 cm^{-1} at room temperature.

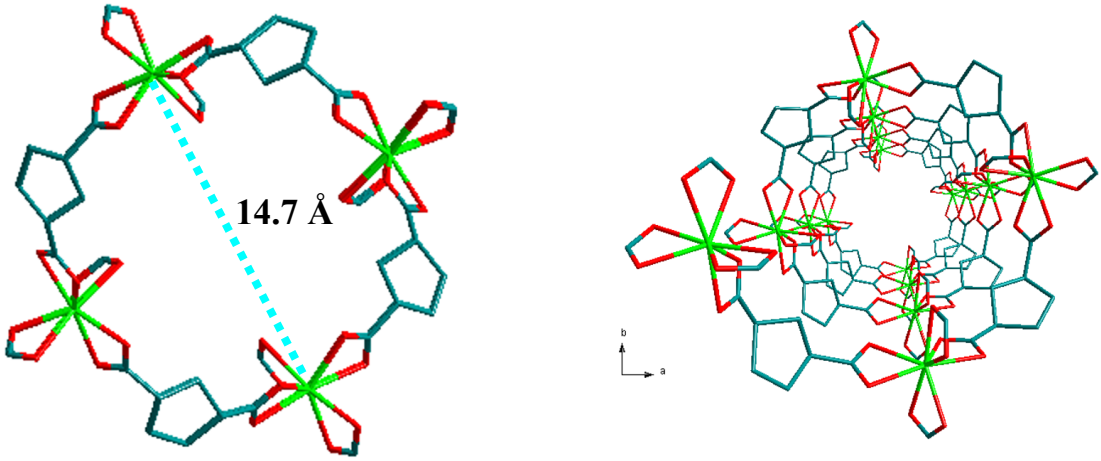

Fig. S3. View the 8-MR channel along the *c* axis.

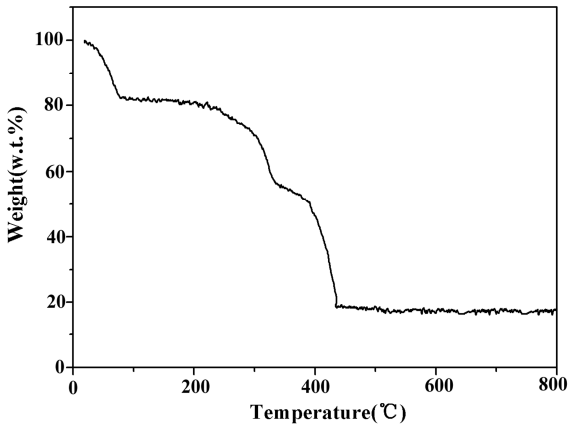

Fig. S4. Thermogravimetric curve for **1**.

Table S1 Selected bond lengths [Å] and angles [°] for compound **1**

In(1)-O(1)	2.295(8)	In(1)-O(1)^{d}	2.295(8)
In(1)-O(2)	2.236(8)	In(1)-O(2)^{d}	2.234(13)
In(1)-O(3)^{b}	2.392(8)	In(1)-O(3)^{c}	2.236(8)
In(1)^{a}- O(3)	2.392(7)	In(1)-O(4)^{b}	2.219(9)
In(1)^{a}-O(4)	2.219(9)	In(1)-O(4)^{c}	2.219(9)
O(4)^{b}-In(1)-O(4)^{c}	128.3(4)	O(4)^{b}-In(1)-O(2)^{d}	116.6(3)
O(4)^{c}-In(1)-O(2)^{d}	84.6(3)	O(4)^{b}-In(1)-O(2)	84.6(3)
O(4)^{c}-In(1)-O(2)	116.6(3)	O(2)^{d}-In(1)-O(2)	132.0(4)
O(4)^{b}-In(1)-O(1)	139.5(3)	O(4)^{c}-In(1)-O(1)	84.0(3)
O(2)^{d}-In(1)-O(1)	86.4(3)	O(2)-In(1)-O(1)	56.7(3)
O(4)^{b}-In(1)-O(1)^{d}	84.0(3)	O(4)^{c}-In(1)-O(1)^{d}	139.5(3)
O(2)^{d}-In(1)-O(1)^{d}	56.7(3)	O(2)-In(1)-O(1)^{d}	86.4(3)
O(1)-In(1)-O(1)^{d}	82.3(4)	O(4)^{b}-In(1)-O(3)^{c}	84.4(3)
O(4)^{c}-In(1)-O(3)^{c}	56.1(3)	O(2)^{d}-In(1)-O(3)^{c}	139.0(3)
O(2)-In(1)-O(3)^{c}	81.7(3)	O(1)-In(1)-O(3)^{c}	99.7(3)
O(1)^{d}-In(1)-O(3)^{c}	164.1(3)	O(4)^{c}-In(1)-O(3)^{b}	84.4(3)
O(2)^{d}-In(1)-O(3)^{b}	81.7(3)	O(2)-In(1)-O(3)^{b}	139.0(3)
O(1)-In(1)-O(3)^{b}	164.1(3)	O(1)^{d}-In(1)-O(3)^{b}	99.7(3)
O(3)^{c}-In(1)-O(3)^{b}	82.8(4)	O(4)^{b}-In(1)-O(3)^{b}	56.1(3)

Symmetry transformations used to generate equivalent atoms:

a -y+1/2,x+1/2,z-1/4 b y-1/2,-x+1/2,z+1/4

c -x+1/2,y-1/2,-z+3/4 d y,x,-z+1